# Collinear Order in Frustrated Quantum Antiferromagnet on Square Lattice (CuBr)LaNb$_2$O$_7$

Noriaki OBA[1], Hiroshi KAGEYAMA[1*], Taro KITANO[1], Jun YASUDA[1], Yoichi BABA[1],
Masakazu NISHI[2], Kazuma HIROTA[2], Yasuo NARUMI[2], Masayuki HAGIWARA[3],
Koichi KINDO[2,3], Takashi SAITO[4], Yoshitami AJIRO[1,5] and Kazuyoshi YOSHIMURA[1]

[1]*Department of Chemistry, Graduate School of Science, Kyoto University, Kyoto 606-8502*
[2]*Institute for Solid State Physics, University of Tokyo, Kashiwa, Chiba 277-8581*
[3]*Center for Quantum Science and Technology under Extreme Conditions, Osaka University,*
*Toyonaka, Osaka 560-8531*
[4]*Institute for Chemical Research, Kyoto University, Uji, Kyoto 611-0011*
[5]*CREST, Japan Science and Technology Agency (JST)*

Magnetic susceptibility, heat capacity, high-field magnetization and neutron diffraction measurements have been performed on a two-dimensional $S = 1/2$ square-lattice system (CuBr)LaNb$_2$O$_7$, prepared by a topotactic ion-exchange reaction of a nonmagnetic double-layered perovskite RbLaNb$_2$O$_7$. (CuBr)LaNb$_2$O$_7$ exhibits a second-order magnetic transition at 32 K, in marked contrast to a spin-singlet nature for its Cl-based counterpart (CuCl)LaNb$_2$O$_7$, despite nearly identical structural parameters. The magnetic structure is a novel collinear antiferromagnetic (CAF) ordering characterized by a modulation vector $\boldsymbol{q} = (\pi, 0, \pi)$ with a reduced moment of $0.6\mu_B$. Mixed ferromagnetic nearest-neighbor ($J_1$) and antiferromagnetic second-nearest-neighbor ($J_2$) interactions are of comparable strength ($J_1/k_B = -35.6$ K and $J_2/k_B = 41.3$ K), placing the system in a more frustrated region of the CAF phase than ever reported.

Quantum fluctuations that are expected to develop near quantum critical points are recognized as primary sources of unconventional phenomena found in condensed matter physics and have been central to intensive research studies. In particular, frustrated square-lattice $S = 1/2$ Heisenberg antiferromagnets with the nearest-neighbor exchange constant $J_1$ and second-nearest-neighbor exchange constant $J_2$, referred to as the antiferromagnetic (AF) $J_1$–$J_2$ model [Fig. 1(b)], have received considerable attention, especially due to the discovery of high-$T_c$ superconducting cuprates whose undoped parent materials are $S = 1/2$ square-lattice antiferromagnets. There are indeed a great deal of controversial theoretical calculations on the AF $J_1$–$J_2$ model,[1–3] but the general consensus is that there exist several interesting phases as a function of the ratio $\alpha = J_2/J_1$; increasing $\alpha$ results in the quantum phase transition from the $\boldsymbol{q} = (\pi, \pi)$ Néel antiferromagnetic (NAF) state to the quantum spin-liquid (QSL) state around $\alpha \sim 0.5$, and further increasing $\alpha$ drives an order by disorder stabilizing the $\boldsymbol{q} = (\pi, 0)$ or $(0, \pi)$ collinear antiferromagnetic (CAF) state, with spins aligned ferromagnetically along the $b$ axis and antiferromagnetically along the $a$ axis, or *vise versa*. Shannon et al. extended the phase diagram to the ferromagnetic (F) $J_1$ ($< 0$) regime, predicting a new gapless QSL state for a region around $\alpha \sim -0.5$ in the F $J_1$–$J_2$ regime, as summarized in Fig. 1(c).[4,5]

On the other hand, only a limited number of compounds were discovered experimentally as prototypes, but relatively large values of $\alpha$ indicating weak frustration were obtained: $\alpha = 3.5, 2.5,$ and $-1.64$ for Li$_2$VOSiO$_4$,[6–8] Li$_2$VOGeO$_4$,[6] and Pb$_2$VO(PO$_4$)$_2$,[9,10] respectively. These are far above the

critical ratio $|\alpha_c| \sim 0.5$ [see Fig. 1(c)], and as theoretically expected, the occurrence of CAF ordering was detected at low temperatures. For probing enhanced quantum fluctuations, new prototype compounds with much stronger frustration are awaited. Low-temperature syntheses may offer promising routes to innovate low-dimensional magnetic compounds, as nonequilibrium phases that are not produced by ordinary solid-state reactions but remain stable under ambient conditions. In fact, reacting a double-layered *nonmagnetic* Dion–Jacobson phase RbLaNb$_2$O$_7$ with Cu$X_2$ yields a perovskite/metal halide intergrowth structure (Cu$X$)LaNb$_2$O$_7$ ($X =$ Cl, Br), where the interlayer Rb$^+$ ions are replaced by the [Cu$X$]$^+$ layer with an $S = 1/2$ square lattice, as shown in Fig. 1(a).[11] We have recently reported that the ground state of (CuCl)LaNb$_2$O$_7$ is described by the QSL, where no long-range order exists down to 20 mK and the spin-singlet ground state is separated from the triplet excited states by a gap of 2.3 meV.[12,13] Moreover, fascinating features have been observed in (CuCl)LaNb$_2$O$_7$, including the localized nature of triplet excitations (possibly as a consequence of competition between $J_1$ and $J_2$), the presence of an excitation at 5.0 meV presumably consisting of several elementary triplets, and an anomalously small critical field ($\sim$10 T) implying the existence of yet unknown states. This letter is motivated by the aforementioned theoretical evolutions for the $J_1$–$J_2$ model and unusual magnetic properties in (CuCl)LaNb$_2$O$_7$. We will demonstrate the magnetic properties of isostructural (CuBr)-LaNb$_2$O$_7$ synthesized by a similar method, and discuss the results in terms of the F $J_1$–$J_2$ model.

The synthesis of (CuBr)LaNb$_2$O$_7$ is expressed by the following ion-exchange reaction:

*E-mail: kage@kuchem.kyoto-u.ac.jp
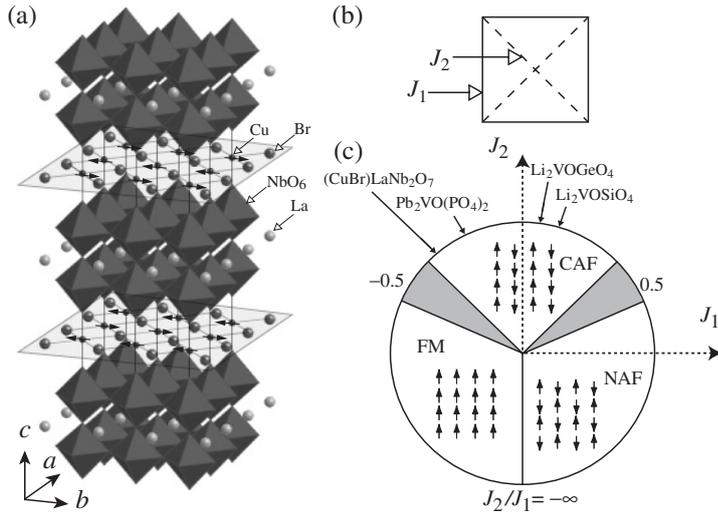
Fig. 1. (a) Schematic representation of crystal and magnetic structures for (CuBr)LaNb$_2$O$_7$. Spins on the Cu$^{2+}$ ions point to the *b*-axis. (b) $J_1$–$J_2$ model on square lattice. (c) General phase diagram for $J_1$–$J_2$ model,[4] where FM, NAF and CAF denote, respectively, $(0,0)$ F, $(\pi,\pi)$ NAF and $(\pi,0)$ CAF phases. The shaded areas correspond to the QSL phases.[4,5] The locations of (CuBr)LaNb$_2$O$_7$, Pb$_2$VO(PO$_4$)$_2$,[9] Li$_2$VOGeO$_4$,[6] and Li$_2$VOSiO$_4$[6] on the phase diagram are indicated by the arrows.

$$RbLaNb_2O_7 + CuBr_2 \rightarrow (CuBr)LaNb_2O_7 + RbCl. \quad (1)$$

The mother compound RbLaNb$_2$O$_7$ was prepared via a conventional high-temperature route, using Rb$_2$CO$_3$ (99.9%), La$_2$O$_3$ (99.99%), and Nb$_2$O$_5$ (99.99%) as starting reagents. RbLaNb$_2$O$_7$ was then mixed with a two-fold molar excess of ultradry CuBr$_2$ (99.9%) and pressed into pellets inside a dry box (<1 ppm O$_2$/H$_2$O). The reaction in eq. (1) was carried out in sealed, evacuated (<10$^{-3}$ Torr) Pyrex tubes at 320 °C for 7 d.[14] The final product was washed with distilled water to eliminate the excess CuBr$_2$ and RbBr, and dried at 120 °C. An X-ray diffraction study confirmed the tetragonal symmetry with room-temperature cell constants $a = 3.9025$ Å and $c = 11.7168$ Å, in good agreement with those previously reported.[11] Energy dispersive spectroscopy (EDS) gave the stoichiometric composition of the final product, assuring complete ion-exchange reactions.

The magnetic susceptibility was studied using a superconducting quantum interference device (SQUID) magnetometer (Quantum Design, MPMS) in the temperature range of $T = 2$–$300$ K in a magnetic field $H = 0.1$ T. High-field magnetization measurements up to 65 T were conducted using a pulse magnet installed at Osaka University. A specific-heat measurement was performed by the heat-relaxation method in a $T$-range from 3.5 to 100 K in the absence of magnetic field using a QD-PPMS at the Institute for Chemical Research, Kyoto University. A hand-pressed pellet was attached to an alumina platform by a small amount of Apiezon N grease. Neutron powder diffraction experiments were conducted using the IMR-HERMES diffractometer (T1-3) and the ISSP-PONTA triple-axis spectrometer (5G), both installed at the JRR-3M reactor of the Japan Atomic Energy Agency (JAEA), Tokai. For the measurements at 5G, a polycrystalline sample of 10 g mass was placed into a vanadium cylinder and neutrons with a wavelength of 2.3618 Å were obtained by the (002) reflection of pyrolytic graphite (PG), and a horizontal collimation of open-40′-sample-80′-80′ in combination with a PG filter placed before the sample to eliminate higher-order beam contaminations.

In Fig. 2, we compare the temperature dependence of the magnetic susceptibility $\chi(T)$ of (CuBr)LaNb$_2$O$_7$ with that of
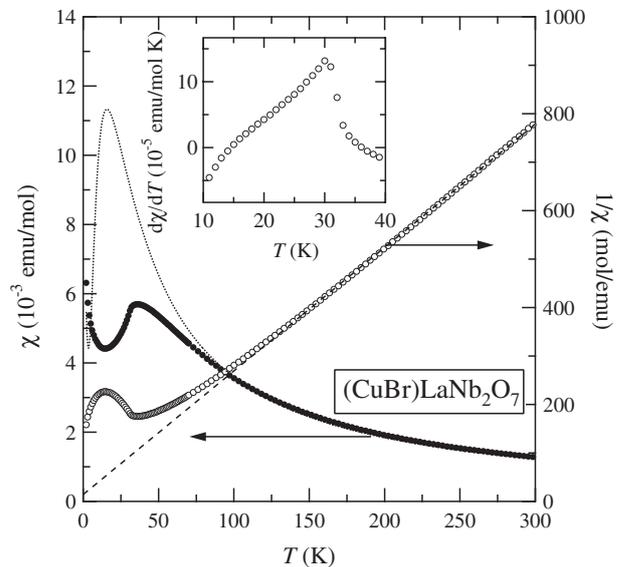


Fig. 2. Magnetic susceptibility $\chi$ (solid circles) and inverse susceptibility $1/\chi$ (open circles) of (CuBr)LaNb$_2$O$_7$ measured at 0.1 T. The broken line is a fit to the Curie–Weiss law. The $\chi(T)$ of (CuCl)LaNb$_2$O$_7$ having the QSL ground state is plotted for comparison purposes by the dotted line.[12] The inset shows the differential susceptibility d$\chi$/d$T$ to illustrate the anomaly at $T_N$.

(CuCl)LaNb$_2$O$_7$.[12] At high temperatures above 100 K, the two lines nearly coincide with respect to each other, from which it is readily determined that the sum of the exchange constants (i.e., $J_1 + J_2$) is of the same order of magnitude for both compounds. The fit of the bromine data with the Curie–Weiss formula $\chi(T) = C/(T - \theta)$ resulted in $\theta = -5.1 \pm 0.5$ K, where $C$ and $\theta$ [$= -(J_1 + J_2)/k_B$] represent the Curie constant and the Weiss temperature. It is close to the value obtained for the chlorine sample ($\theta = -9.6$ K). The verification of the completion of the ion-exchange reaction is made again by finding $C = 0.393$ emu/(K mol), which is quite reasonable for 1 mol of Cu$^{2+}$ ions in (CuBr)LaNb$_2$O$_7$.

Despite the apparent similarity between the high-$T$ behaviors of $\chi(T)$ of the two samples, a marked difference becomes discernible for $T < 100$ K. $\chi(T)$ for $X =$ Br shows a round maximum at $T_M = 36.0$ K, which is expected for

low-dimensional magnetic systems but is much higher than $T_M = 16.0$ K for $X = $ Cl.[12] This fact is an implication that the former has greater magnitudes of both $J_1$ and $J_2$, which will be confirmed later by the magnetization curve. The ratio $T_M/|\theta|$ is equal to 7.06 and is considerably larger than 0.935 expected for the nonfrustrated case.[15] It implies, together with the structural characteristics of the Cu$X$ layer, that for $X = $ Br, $J_2$ is AF while $J_1$ is F, as in the case for $X = $ Cl[12,13] and for $Pb_2VO(PO_4)_2$.[9]

$\chi(T)$ for the bromine sample reveals a tiny kink at $\sim 30$ K pointing to a transition into a magnetically ordered state. It is better shown if one plots the derivative susceptibility $d\chi/dT$, as seen in the inset of Fig. 2. The upturn in $\chi(T)$ at around 15 K is attributed to impurities or defects and corresponds approximately to what one would expect for 1.5% of noninteracting paramagnetic one-half spins. The subtraction of the extrinsic term resulted in a finite susceptibility $\sim 3 \times 10^{-3}$ emu/mol at 0 K. This is in stark contrast to the thermally activated behavior in the chlorine sample, i.e., $\chi \to 0$ as $T \to 0$. The heat capacity divided by temperature
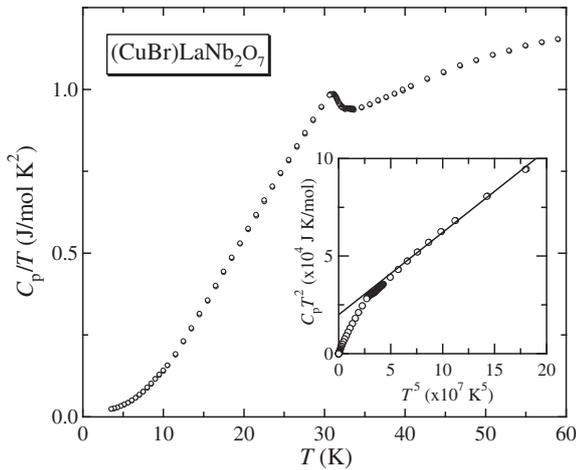


Fig. 3. Temperature dependence of $C_p/T$ for $(CuBr)LaNb_2O_7$ showing magnetic ordering at 32 K. The inset shows the $C_pT^2$ vs $T^5$ plot, where the solid line represents the linear fit between 35 and 48 K.

$C_p/T$ (Fig. 3) reproduces the anomaly at a similar temperature 32.0 K ($= T_N$). The transition is nearly of second order, as inferred from the small anomaly around $T_N$ without hysteresis. No further anomaly in the $C_p/T$ vs $T$ plot is seen down to 2 K, the lowest $T$ examined in the present study.

Neutron diffraction analysis allows one to directly establish the spin-ordering structure as well as the magnitude of the ordered moment. We show, in Figs. 4(a) and 4(b), powder neutron diffraction patterns obtained at 5G for temperatures below and above $T_N$, and, in Figs. 4(c) and 4(d), the corresponding difference plots. Note that the experiments using T1-3 essentially gave the same results. The appearance of new reflections below $T_N$ is due to the breakdown of translational symmetry and is firm evidence for long-range magnetic ordering. The angular positions of the observed magnetic Bragg peaks reveal that the magnetic unit cell has a magnetic ordering vector $q = (\pi, 0, \pi)$. It is natural to consider that the magnetic structure is such that layers of the CAF type stack along the $c$-axis in a staggered manner, as illustrated in Fig. 1(a). We found that $(1/2, 0, 1/2)$ and $(1/2, 0, 3/2)$ reflections have nearly the same magnetic structure factors, implying that the spins point parallel to the $b$-axis, which is supported by the fact that reflections such as $(1/2, 1, 1/2)$ are not visible within the experimental resolution. We would like to stress here that $(CuBr)LaNb_2O_7$ is a second experimental example of the CAF phase in the $S = 1/2$ square-lattice systems having mixed F and AF exchange couplings.[10]

The inset of Fig. 4 shows that the intensity of the $(1/2, 0, 1/2)$ reflection decreases with increasing $T$ and continuously becomes zero at 32 K, which is ascribed to the onset of the second-order-like transition in accordance with the result for the heat capacity. The critical exponent $\beta$ for the magnetization below $T_N$ takes a value close to that expected for a three-dimensional Heisenberg model (0.345) (see the inset of Fig. 3). Once given the magnetic structure in Fig. 1(a), one can determine the ordered magnetic moment $m$ from the intensities of the observed magnetic reflections, which are proportional to the square of $m$. We obtain a reduced moment ($0.60 \pm 0.11 \mu_B$) which is indeed
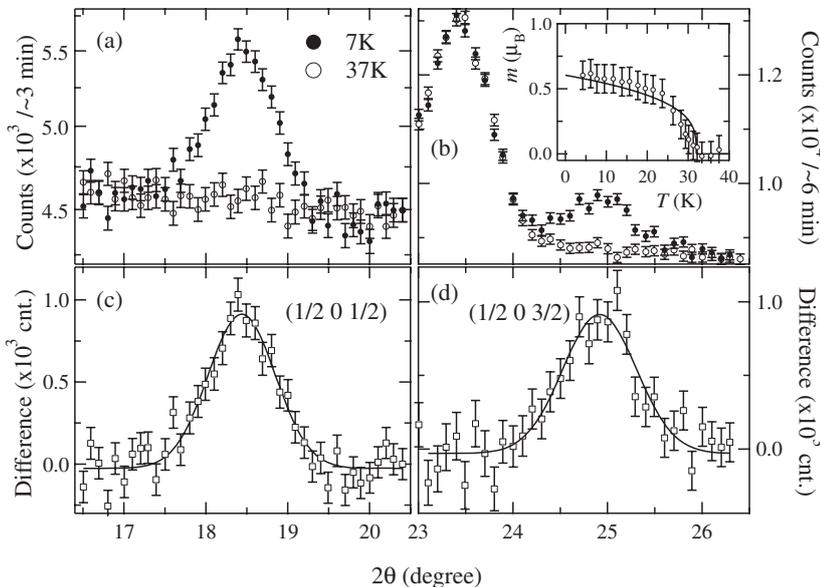


Fig. 4. (a) Powder neutron diffraction profile for $2\theta = 16$–$20.5°$ for $(CuBr)LaNb_2O_7$ at 7 K (solid), 37 K (open) and (c) difference plot, demonstrating $(1/2, 0, 1/2)$ reflection. (b), (d) Same plot for $2\theta = 23$–$26.5°$, demonstrating $(1/2, 0, 3/2)$ reflection. The solid lines in (c) and (d) represent Gaussian fits. Inset: temperature dependence of magnetic moment $m$. The line is fitted with a power law: $m = 0.60(1 - T/T_N)^\beta$ with $\beta = 0.30$.
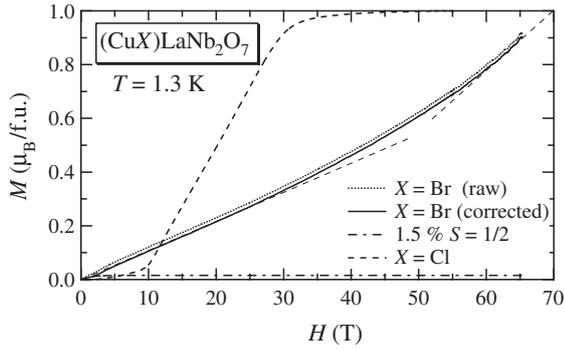
Fig. 5. Dotted line: magnetization of $(CuBr)LaNb_2O_7$ measured at 1.3 K. Dot-broken line: impurity term, given by Brillouin function for 1.5% of noninteracting $S = 1/2$ spins at 1.3 K. Solid line: corrected magnetization of $(CuBr)LaNb_2O_7$ after subtraction of above impurity term. Broken line: magnetization of $(CuCl)LaNb_2O_7$.[13]

comparable to that expected from the nonfrustrated two-dimensional square lattice model ($0.65\mu_B$).[16]

Shown in Fig. 5 is the magnetization $M(H)$ measured at 1.3 K, in which the raw data was corrected by subtracting the contribution from the impurities/defects observed in the magnetic susceptibility. Here, thermal fluctuations in the magnetization are negligible at this temperature, since there is little difference between the 1.3 and 4.2 K curves. For $0 < H < 30$ T, $M(H)$ varies almost linearly with $H$. The linear field dependence is subsequently followed by non-linear growth. $M(H = 65$ T$)$ is 95% of the saturation magnetization. The upward curvature should be a result of the gradual suppression of zero-point oscillations by the external field and is expected to be observed in the framework of spin-wave theory for frustrated and non-frustrated AF square-lattice systems for all fields below the saturation field $H_s$.[17,18] Possibly, the linear field dependence is an intrinsic nature for the frustrated F square-lattice system. It is worth noting that a 1/2 plateau corresponding to a state with up-up-up-down spin order has been theoretically suggested in the frustrated CAF regime for the AF square lattice.[19] The absence of the plateau in our experiment might be due to the fact that we deal with the F square lattice.

Let us hereafter discuss the question of whether or not a sizable frustration is present in this compound by utilizing various methods. The magnetization curve at sufficiently low temperatures can be taken full advantage of to unambiguously determine the exchange constants, and hence measure the frustration $\alpha$. We estimate $H_s$ from a linear extrapolation of the $M$–$H$ curve. The obtained field of 70 T is much larger than 30.1 T for the chlorine sample.[13] On the basis of the $J_1$–$J_2$ model, the saturation field is given by $H_s = 2(J_1 + 2J_2)/g\mu_B$ for the CAF phase. By assuming $(J_1 + J_2)/k_B = 5.1$ K ($= |\theta|$), we determine $J_1/k_B = -35.6$ K and $J_2/k_B = 41.3$ K and hence $|\alpha| = 1.10$, which is the smallest among the compounds with a CAF state and places the present compound in the most frustrated region on the phase diagram of the $J_1$–$J_2$ model.

The evaluation of $\alpha$ can also be discussed using the high-temperature expansions (HTEs) of heat capacity studied by Misguich et al.,[20] who predict that at high temperatures, the magnetic heat capacity of the $J_1$–$J_2$ model

behaves as $C_M \sim 0.375R(J_1{}^2 + J_2{}^2)/(k_BT)^2$ [$R = 8.314$ J/(mol K)]. Since there is a $T^3$ contribution from phonons at low temperatures, $C_pT^2$ is plotted against $T^5$ [Fig. 3 (inset)]. A linear behavior is seen for $35 < T < 48$ K. Then, the linear extrapolation to $T = 0$ gives $(J_1{}^2 + J_2{}^2)/k_B{}^2 \sim 6400$ K$^2$ which is larger than that obtained above roughly by a factor of 2, but may be acceptable in view of the difficulty in extracting the phonon contribution from the raw data, owing to the lack of a nonmagnetic isostructural compound.

A problem arises when a quantitative comparison between $(CuBr)LaNb_2O_7$ and $(CuCl)LaNb_2O_7$ is made with respect to $\alpha$. The estimated value of 4.50 ($J_1/k_B = -2.74$ K and $J_2/k_B = 12.34$ K) for $(CuCl)LaNb_2O_7$[13] indicates that it is less frustrated and should be in the CAF region. From this viewpoint, the appearance of the spin-singlet formation in $(CuCl)LaNb_2O_7$ is an interesting puzzle to be solved in the future. Further studies, in particular those on the solid solution between the end members, would offer better understanding of the relationship between the QSL and CAF phases, which will be published elsewhere.

In conclusion, we demonstrated that the two-dimensional $S = 1/2$ square-lattice system $(CuBr)LaNb_2O_7$ exhibits the long-range magnetic ordering of the CAF type at 32 K, in marked contrast to the QSL behavior in $(CuCl)LaNb_2O_7$. Strong competition between the F $J_1$ and AF $J_2$ interactions is suggested. The proximity of the CAF state of $(CuBr)LaNb_2O_7$ to the QSL state next to the F state might be relevant to the spin-singlet formation in $(CuCl)LaNb_2O_7$. We wish to point out that there have already been numerous studies on $^3$He with competing F and AF multiple spin-exchange processes and on the doped colossal magneto-resistive (CMR) manganites with competing F kinetic and AF repulsive exchange energies. On the contrary, little is known about frustrated ferromagnets in quantum spin systems. $(CuX)LaNb_2O_7$ should serve in the development of such systems.

1)  N. Read and S. Sachdev: Phys. Rev. Lett. **62** (1989) 1694.
2)  M. P. Gelfand, R. R. P. Singh and D. A. Huse: Phys. Rev. B **40** (1989) 10801.
3)  F. Becca and F. Mila: Phys. Rev. Lett. **89** (2002) 037204.
4)  N. Shannon, B. Schmidt, K. Penc and P. Thalmeier: Eur. Phys. J. B **38** (2004) 599.
5)  N. Shannon, T. Momoi and P. Sindzingre: Phys. Rev. Lett. **96** (2006) 027213.
6)  R. Melzi, P. Carretta, A. Lascialfari, M. Mambrini, M. Troyer, P. Mittlet and F. Mila: Phys. Rev. Lett. **85** (2000) 1318.
7)  A. Bombardi, J. Rodriguez-Carvajal, S. Di Matteo, F. de Bergevin, L. Paolasini, P. Carretta, P. Millet and R. Caciuffo: Phys. Rev. Lett. **93** (2004) 027202.

8)  R. Melzi, S. Aldrovandi, F. Tedoldi, P. Carretta, P. Millet and F. Mila: Phys. Rev. B **64** (2001) 024409.

9)  E. E. Kaul, H. Rosner, N. Shannon, R. V. Shpanchenko and C. Geibel: J. Magn. Magn. Mater. **272–276** (2004) 922.

10)  M. Skoulatos, J. P. Goff, N. Shannon, E. E. Kaul, C. Gaibel, A. P. Murani, M. Enderle and A. R. Wildes: Abstr. Int. Conf. Magnetism, Kyoto, 2006, p. 409.

11)  T. A. Kodenkandath, J. Lalena, W. L. Zhou, E. Carpenter, C. Sangregorio, A. Falster, W. Simmons, C. O'Connor and J. B. Wiley: J. Am. Chem. Soc. **121** (1999) 10743.

12)  H. Kageyama, T. Kitano, N. Oba, M. Nishi, S. Nagai, K. Hirota, L. Viciu, J. B. Wiley, J. Yasuda, Y. Baba, Y. Ajiro and K. Yoshimura: J. Phys. Soc. Jpn. **74** (2005) 1702.

13)  H. Kageyama, J. Yasuda, T. Kitano, K. Totsuka, Y. Narumi, M. Hagiwara, K. Kindo, Y. Baba, Y. Ajiro and K. Yoshimura: J. Phys. Soc. Jpn. **74** (2005) 3155.

14)  $CuBr_2$ generates higher bromine pressure during the reaction in eq. (1) than in the case of $CuCl_2$. We worked with Pyrex tubes that have a 12 mm outer diameter and a wall thickness of 1.5 mm and that are sealed to give a tube length ranging from 13 to 17 cm. The maximum weight of reactants for each tube was set to less than 1.5 g.

15)  J.-K. Kim and M. Troyer: Phys. Rev. Lett. **80** (1998) 2705.

16)  H. J. Schulz, T. A. L. Ziman and D. Poilblanc: J. Phys. I **6** (1996) 675.

17)  M. E. Zhitomirsky and T. Nikuni: Phys. Rev. B **57** (1998) 5013.

18)  M. S. Yang and K. H. Mütter: Z. Phys. B **104** (1997) 117.

19)  M. E. Zhitomirsky, A. Honecker and O. A. Petrenko: Phys. Rev. Lett. **85** (2000) 3269.

20)  G. Misguich, B. Bernu and L. Pierre: Phys. Rev. B **68** (2003) 113409.